

Similarity Theory of the Buoyantly Interactive Planetary Boundary Layer with Entrainment

MARTIN I. HOFFERT

Department of Applied Science, New York University, New York, N. Y. 10003

Y. C. SUD

Math Analysis Group, GTE Information Systems, Goddard Institute for Space Studies, New York, N. Y. 10025

(Manuscript received 6 February 1975, in revised form 20 July 1976)

ABSTRACT

A similarity model is developed for the vertical profiles of turbulent flow variables in an entraining turbulent boundary layer of arbitrary buoyant stability. In the general formulation the vertical profiles, internal rotation of the velocity vector, discontinuities or jumps at a capping inversion and bulk aerodynamic coefficients of the boundary layer are given by solutions to a system of ordinary differential equations in the similarity variable $\eta = z/h$, where h is the physical height or thickness, where the system includes six parameters associated with surface roughness, buoyant stability of the turbulence near the surface, Coriolis effects, baroclinicity and stability of the air mass above the boundary layer. To close the system a new formulation for buoyantly interactive eddy diffusivity in the boundary layer is introduced which recovers Monin-Obukhov similarity near the surface and incorporates a hypothesis accounting for the observed variation of mixing length throughout the boundary layer.

The model is tested in simplified versions which depend only on roughness, surface buoyancy and Coriolis effects by comparison with Clarke's planetary boundary layer wind and temperature profile observations, Arya's measurements of flat-plate boundary layers in a thermally stratified wind tunnel, and Lenschow's observations of profiles of terms in the turbulent kinetic energy budget of convective planetary boundary layers. On balance, the simplified model reproduced the trend of these various observations and experiments reasonably well, suggesting that the full similarity formulation be pursued further.

1. Introduction

The planetary boundary layer (PBL), formed by the interaction of atmospheric motions with the earth's surface, is a turbulent region of variable thickness [$O(1 \text{ km})$] across which momentum, heat and moisture are transferred by turbulent mixing. PBL turbulence is generated partly by wind shears and partly by buoyancy fluxes associated with surface heating.

When the surface is warmer than the air above turbulent fluctuations are generally more intense (buoyantly unstable or "convective" turbulence). When it is cooler fluctuations are suppressed or even extinguished (buoyantly stable turbulence). Observations over land and sea surfaces confirm the buoyantly interactive PBL is the general case (Clarke, 1970; Clarke *et al.*, 1971; Sarachik, 1974), although buoyantly neutral Ekman-layer-like structures, such as those analyzed by Blackadar (1962), are also observed under adiabatic conditions and are an important limit in any general theory of the buoyantly interactive PBL. Over land diurnal heating and cooling cycles gives rise to boundary layer structures which are continually evolving. Typically, an inversion-capped convective

PBL forms near sunrise, grows during the day by entraining mass from the overlying laminar layer (Tennekes, 1973; Carson, 1973), and eventually dissipates and relaminarizes in late afternoon when the surface heat flux changes sign and a "new" shallow stable PBL forms near the ground (Businger, 1973). Unstable, neutral and stable PBL's are all possible over the oceans, but the high heat capacity of the sea surface tends to damp out diurnal cycles.

In most models of the buoyantly interactive PBL the objective is to find the possibly unsteady turbulent-mean flow distribution in the vertical above a fixed point, and corresponding values of surface stress, heat flux and evaporation, in terms of boundary conditions applied at the surface and above the PBL. The central problem is finding the turbulent fluctuations or modeling their moments in terms of turbulent-mean fluid properties (the "closure" problem). Perhaps the most general approach is Deardorff's (1974), who finds the one-dimensional mean flow by horizontally averaging a numerical finite-difference solution to the unsteady three-dimensional problem wherein the larger turbulent eddies are computed explicitly and subgrid turbulence

is modeled. Orlanski *et al.* (1974) have developed a two-dimensional model which is similar in concept. In contrast are the ensemble-mean PBL closure models of Wyngaard and Coté (1974) and Mellor and Yamada (1974) in which turbulent covariances or moments appear as dependent variables. Such higher moment closure is not a unique solution to the turbulence problem, but the theories of Donaldson (1973) and others and more recently of Lumley and Khajeh-Nouri (1974) on which the PBL models are based, have given good results and are more economical than explicit turbulence calculations. Finally, there are the eddy diffusivity mixing-length models generalized to the buoyantly interactive case by Bobileva *et al.* (1967), Businger and Arya (1974), Clarke (1974) and Wippermann (1974). Again, these are not unique solutions to the turbulence problem but must be judged on the basis of their internal consistency, ability to reproduce observations and computational economy.

Our purpose in this paper is to develop a relatively simple model of buoyantly interactive PBL structure which accounts for most of the observational features of interest in boundary layer meteorology. There are two key steps in the development of the model. The first is a transformation of the one-dimensional, unsteady, partial differential equations for PBL mean quantities to ordinary differential equations by introducing a similarity variable, the PBL height-normalized vertical coordinate. The second is a new generalization of the eddy diffusivity for buoyantly interactive boundary layers which is consistent with observed Monin-Obukhov similarity in the surface layer and also reflects the observed variation of turbulence scale through the PBL as a whole. The model describes the structure of the entire PBL from the surface where the mean velocity goes to zero to the edge which may be taken coincident with the base of a capping inversion. The model permits inclusion of such edge discontinuities in a self-consistent manner. Moreover, the bulk aerodynamic coefficients emerge as by-products of the similarity structure solutions, in contrast to asymptotic matching methods based on mating inner and outer profiles at some interior point, and fitting observational data to the implied functional forms to get the exchange coefficients (Sheppard, 1970; Csanady, 1972; Melgarejo and Deardorff, 1974; Zilitinkevich and Deardorff, 1974; Zilitinkevich, 1975a).

2. Governing equations

We consider the unsteady turbulent boundary layer of thickness h which develops as wind blows over a heated or cooled surface. We make the usual geophysical boundary layer assumption that Coriolis forces from the rotating earth contribute to the momentum balance and allow for the adiabatic lapse rate's contribution to temperature change across the

layer by using potential temperature in the energy balance. The model will, however, recover the limit of a shallow diabatic turbulent boundary layer, say, in a wind tunnel. Radiative absorption and phase change are neglected.

The relevant flow variables are velocity $\mathbf{U} = (u, v, w) = (\bar{u} + u', \bar{v} + v', \bar{w} + w')$, potential temperature $\theta = \bar{\theta} + \theta'$ and specific humidity $q = \bar{q} + q'$, where overbars denote Reynolds averages and primes denote fluctuations. The flow is primarily along the horizontal mean wind \bar{u} , $\bar{v} (\gg \bar{w})$; turbulent mixing is mainly vertical by the Reynolds stress components $\tau_x \equiv -\rho \overline{u'w'}$ and $\tau_y \equiv -\rho \overline{v'w'}$; and the sensible heat flux $F \equiv \rho C_p \overline{w'\theta'}$ and the water vapor flux $E \equiv \rho \overline{w'q'}$, where ρ is the density and C_p the constant-pressure specific heat of air. In the Boussinesq approximation for air, density fluctuations relate to fluctuations in *virtual* potential temperature $\theta_v \approx \theta(1 + 0.608q)$ by $\rho'/\bar{\rho} \approx -\theta_v'/\bar{\theta}$. Ordinarily we take $\theta \approx \theta_v$, except when differences or fluctuations are involved. An important quantity in turbulent, buoyantly interactive flows is the vertical buoyancy flux

$$F_b \equiv -C_p \bar{\theta} \overline{\rho'w'} \approx \rho C_p \overline{w'\theta_v'} \approx F + 0.608 C_p \bar{\theta} E,$$

where F , E and F_b are positive upward, and buoyantly unstable, neutral and stable conditions correspond to F_b positive, zero and neutral, respectively. Other moments of interest are the kinetic energy per unit mass in turbulent fluctuations $\bar{e} \equiv (\overline{u'^2 + v'^2 + w'^2})/2$, the vertical flux of turbulent kinetic energy $G \equiv \rho (\overline{w'e'}) + \overline{w'p'}$ including a component carried by pressure fluctuations, and the turbulent dissipation rate per unit mass

$$\epsilon \equiv \frac{1}{2} \nu \sum_{i,j} \overline{(\partial u'_i / \partial x_j + \partial u'_j / \partial x_i)^2}.$$

We take the governing equations for this problem as the definitions of turbulent eddy diffusivity of momentum K_m (assumed independent of the horizontal wind direction) and of buoyancy K_H [assumed equal to that of sensible heat and humidity (see Dyer, 1967)], the conservation equations for both horizontal components of mean momentum, and the conservation equations for buoyancy flux (the sum of the mean energy and humidity conservation equations) and turbulent kinetic energy (see Monin and Yaglom, 1971, p. 400):

$$0 = \partial \bar{u} / \partial z - \tau_x / (\rho K_m), \tag{1a}$$

$$0 = \partial \bar{v} / \partial z - \tau_y / (\rho K_m), \tag{1b}$$

$$0 = \partial \bar{\theta}_v / \partial z + F_b / (\rho C_p K_H), \tag{1c}$$

$$\rho d\bar{u} / dt = \partial \tau_x / \partial z + \rho f(\bar{v} - v_g), \tag{1d}$$

$$\rho d\bar{v} / dt = \partial \tau_y / \partial z - \rho f(\bar{u} - u_g), \tag{1e}$$

$$\rho d\theta_v / dt = -\partial F_b / \partial z, \tag{1f}$$

$$0 = -(\rho d\bar{e}/dt + \partial G/\partial z) + (\tau_x \partial \bar{u}/\partial z + \tau_y \partial \bar{v}/\partial z) + (gF_b/(C_p \theta_v)) - (\rho \epsilon), \quad (2)$$

"transport"
shear production
buoyant production
dissipation

where $f = 2\Omega \sin\phi$ is the Coriolis parameter with Ω the earth's angular velocity and ϕ the latitude, $(u_\sigma, v_\sigma) \equiv (\rho f)^{-1}(-\partial p/\partial y, \partial p/\partial x)$ is the geostrophic wind, and g is the gravitational acceleration.

It is convenient at this point to impose lower boundary conditions on (1a)–(1f) at the aerodynamic roughness height z_0 —a property of surface topography over land and formally the point in a turbulent boundary layer above the nominal surface where the mean velocity may be considered to vanish:

$$\left. \begin{aligned} \bar{u} &= 0, \quad \bar{v} = 0, \quad \bar{\theta}_v = \bar{\theta}_{vs} \\ \tau_x &= \tau_s, \quad \tau_y = 0, \quad F_b = F_{bs}; \quad \text{at } z = z_0 \end{aligned} \right\} \quad (3)$$

In this paper the subscript s denotes "surface" conditions at $z = z_0$ and the subscript h denotes "edge" conditions at $z = h$ immediately below any edge discontinuities such as inversion lids. Notice in (3) that we have adopted an x, y horizontal coordinate system in which the surface stress is parallel to the x axis so the y component vanishes at the surface identically.

Generally, both components of horizontal momentum are retained in PBL models since the effect of the geostrophic departure terms in (1d) and (1c) is to rotate the stress and velocity vectors through an angle $\Psi_h = \tan^{-1}(-v_h/u_h)$ relative to the x axis. The corresponding edge velocity is $(u_h, v_h) = U_h(\cos\Psi_h, -\sin\Psi_h)$, where $U_h = (u_h^2 + v_h^2)^{1/2}$ is the edge wind speed magnitude. In neutral PBL's the edge velocity can usually be taken geostrophic to a good approximation, at least away from the equator, but recent observations of convective PBLs indicate it differs by some value $(\Delta u_h, \Delta v_h) = (u_h^+ - u_h, v_h^+ - v_h)$ at the inversion base (see Deardorff, 1973, and Figs. 5 and 6 of Arya and Wyngaard, 1975). These measurements show that adjustment to geostrophic equilibrium takes place within the inversion and that the velocity above is very nearly geostrophic. Idealizing the inversion lid as a constant-pressure (constant geostrophic wind) discontinuity we may write $(u_{gh}, v_{gh}) = (u_h + \Delta u_h, v_h + \Delta v_h)$. In the absence of velocity jumps the edge velocity may be considered geostrophic and oriented along isobars, and Ψ_h is interpretable in the classical sense of a total cross-isobar turning angle for velocity due to frictional effects.

Under barotropic or horizontally homogeneous conditions the geostrophic wind is constant in magnitude and direction through the PBL. Baroclinically geostrophic wind shears are generated within by the thermal wind relations

$$(\partial u_\sigma/\partial z, \partial v_\sigma/\partial z) \approx (g/f)(-\partial \ln \bar{\theta}_v/\partial y, \partial \ln \bar{\theta}_v/\partial x)$$

(Hess, 1959). Taking $\bar{\theta}_v \approx \langle \bar{\theta}_v \rangle$ as the depth-averaged

potential (or virtual potential) temperature gives constant geostrophic shears and linear profiles $(u_\sigma, v_\sigma) \approx [u_{\sigma h} + (\partial u_\sigma/\partial z)(z-h), v_{\sigma h} + (\partial v_\sigma/\partial z)(z-h)]$. Combining the foregoing relations gives the geostrophic wind profiles in the present model under buoyantly interactive baroclinic conditions:

$$u_\sigma(z) = +U_h \cos\Psi_h + \Delta u_h - [(g/f)\partial \ln \langle \bar{\theta}_v \rangle / \partial y](z-h), \quad (4a)$$

$$v_\sigma(z) = -U_h \sin\Psi_h + \Delta v_h + [(g/f)\partial \ln \langle \bar{\theta}_v \rangle / \partial x](z-h). \quad (4b)$$

The edge velocity jumps are discussed in more detail later in this paper.

In the present formulation we account approximately for an advective contribution to $d\bar{u}/dt$, $d\bar{v}/dt$, $d\bar{\theta}_v/dt$, etc., by defining the total time derivative operator as $d(\)/dt = \partial(\)/\partial t + \langle \bar{\mathbf{U}} \rangle \cdot \nabla(\)$, where $\langle \bar{\mathbf{U}} \rangle$ is the depth-averaged velocity and $\nabla(\)$ the horizontal gradient operator. Consistently, the vertical velocity has a linear distribution; from continuity we get

$$\bar{w}(z) = - \int_0^z \nabla \cdot \langle \bar{\mathbf{U}} \rangle d\bar{z} = w_h z/h, \quad (5)$$

where $w_h = -h \nabla \cdot \langle \bar{\mathbf{U}} \rangle$ is the vertical edge velocity. The evolution of the physical boundary layer height is given by the depth-averaged continuity equation for a turbulent slab of thickness h , entraining laminar air at the top at velocity w_e (Deardorff, 1972; Tennekes, 1973):

$$dh/dt = w_h + w_e. \quad (6)$$

To close the system we shall make use of the turbulent kinetic energy equation (2) to derive expressions for K_m and K_H for the buoyantly interactive ($F_b \neq 0$) case in terms of quantities generated internally by the model and a prescribed distribution of the turbulent mixing length $l_N(z)$ in neutral ($F_b = 0$) boundary layers. In the traditional Prandtl (1925, 1932) mixing length theory used by Blackadar (1962) and others with some success to model a neutral PBL, the momentum eddy diffusivity is given by $K_m = l_N^2 |\partial \bar{\mathbf{U}}/\partial z|$ with $l_N(z) \equiv (|\tau|/\rho)^{1/2} |\partial \bar{\mathbf{U}}/\partial z|^{-1}$ empirically prescribed. Near the surface $l_N = \kappa z$, where $\kappa \approx 0.35$ is von Kármán's constant (Businger *et al.*, 1971); near the edge $l_N = ch$, where we estimate $c \approx 0.052$ from Clarke's (1970) PBL data for near neutral conditions. The interpolation formula

$$l_N(z) = ch \{1 - \exp[-\kappa z/(ch)]\} \quad (7)$$

is adopted here to smoothly match these limiting forms through a neutral boundary layer. More generally, a buoyantly interactive mixing length may be defined in terms of the momentum eddy diffusivity and the turbulence dissipation rate by (Heisenberg, 1948)

$$l(z) \equiv K_m^{1/2} \epsilon^{-1/4}, \quad (8)$$

where a dimensionless coefficient of order unity has been

incorporated in the definition of $l(z)$ for consistency with the Prandtl mixing length theory in the neutral limit (Blackadar, 1962).

Now, eliminating τ_x, τ_y, F_b and ϵ in (2) with the help of (1a,b,c) and (8) and solving for K_m gives a form which applies in the buoyantly interactive case:

$$K_m(z) = \beta^2 l_N^2 [(\partial \bar{u} / \partial z)^2 + (\partial \bar{v} / \partial z)^2]^{\frac{1}{2}} [1 - \alpha(1 + \gamma) \text{Ri}]^{\frac{1}{2}}, \quad (9)$$

where

$$\text{Ri}(z) = [(g/\bar{\theta}_v) \partial \bar{\theta}_v / \partial z] / [(\partial \bar{u} / \partial z)^2 + (\partial \bar{v} / \partial z)^2] \quad (10)$$

is the local gradient Richardson number,

$$\alpha(z) \equiv K_H / K_m \quad (11a)$$

is the local ratio of thermal to momentum eddy diffusivity,

$$\beta(z) \equiv l / l_N \quad (11b)$$

is the local ratio of the buoyantly interactive to the neutral mixing length, and

$$\gamma(z) \equiv -C_p \bar{\theta}_v (\rho d\bar{z}/dt + \partial G / \partial z) / (g F_b) \quad (11c)$$

is the local ratio of turbulent kinetic energy "transport" (local derivative + advection + pressure transport + turbulent diffusion) to buoyant production terms. Expressions resembling (9) are sometimes quoted in the literature with some or all of the coefficients α, β and γ taken constant. We will show later that constant values are inconsistent with surface layer similarity theory. Also to be discussed later is a method for specifying the *closure functions* $\alpha(z), \beta(z)$ and $\gamma(z)$ in terms of the surface buoyancy flux and shear stress.

3. Parameterization and similarity

The basic problem in parameterizing PBL effects in large-scale atmospheric models is expressing the surface stress, sensible heat flux and evaporative flux in terms of known boundary conditions and parameters known from the large-scale model without calculating the detailed PBL structure for each case. Generally considered known if the boundary layer height h is known are the fluid properties above the PBL (and above any edge discontinuities) such as U_h^+, θ_{vh}^+ , etc.; the static stability of the overlying air mass $\partial \theta_v^+ / \partial z$; and the PBL depth-averaged horizontal thermal gradient $\nabla \langle \theta_v \rangle \approx \nabla \langle \theta_{vh}^+ \rangle$. Such parameterizations may take the form of bulk aerodynamic exchange coefficients derived from semi-empirical data correlations or from other considerations (Deardorff, 1972; Bhumralkar, 1976).

In what follows a method is developed for finding the bulk aerodynamic coefficients for drag $C_D \equiv \tau_s / (\rho U_h^2)$, sensible heat transfer $C_H \equiv -F_s / [\rho C_p U_h (\theta_h - \theta_s)]$ and evaporation $C_E \equiv -E_s / [\rho U_h (q_h - q_s)]$ as by-products of the similarity solutions to the governing PBL equations. Consistent with our assumption of the same turbulent diffusivity for sensible heat and water vapor, we take $C_H = C_E$, so the surface buoyancy flux is $F_{bs} \approx F_s$,

$+0.608 C_p \theta_s E_s \approx -\rho C_p U_h (\theta_{vh} - \theta_{vs}) C_H$. Note also that τ_s is generally rotated with respect to U_h by $-\Psi_h$. Accordingly, the parameterization problem may be regarded as specification of C_D, C_H, Ψ_h and the edge discontinuities $\Delta u_h, \Delta v_h, \Delta \theta_{vh}$ (when present) in terms of bulk similarity parameters known or calculable from the large-scale dynamics and boundary conditions. To facilitate the similarity-scale analysis we introduce the usual friction velocity and buoyancy temperature scales

$$u^* \equiv (\tau_s / \rho)^{\frac{1}{2}} = C_D^{\frac{1}{2}} U_h, \quad (12a)$$

$$\theta_v^* \equiv -F_{bs} / (\rho C_p u^*) = C_D^{-\frac{1}{2}} C_H (\theta_{vh} - \theta_{vs}), \quad (12b)$$

and the buoyancy velocity scale

$$w^* \equiv (-ghu^* \theta_v^* / \theta_{vs})^{\frac{1}{2}} = C_H^{\frac{1}{2}} [ghU_h (\theta_{vs} - \theta_{vh}) / \theta_{vs}]^{\frac{1}{2}}, \quad (12c)$$

where θ_v^* is negative in unstable ($\theta_{vs} > \theta_{vh}$) boundary layers, zero in neutral ($\theta_{vs} = \theta_{vh}$) boundary layers and positive in stable ($\theta_{vs} < \theta_{vh}$) boundary layers; w^* is positive in unstable boundary layers and zero in neutral boundary layers.

The turbulent entrainment velocity w_e in (6) plays an important role in the similarity model we are developing here. Deardorff (1974) has developed and tested an interpolation formula for the entrainment velocity in terms of the surface stress and buoyancy flux which can be put in the form

$$w_e = \begin{cases} \frac{1.8w^{*3} \{1 + 1.1(u^*/w^*)^3 [1 - hf / (\kappa u^*)]\}}{(gh^2/\theta_v) \partial \theta_v^+ / \partial z + 9w^{*2} [1 + 0.8(u^*/w^*)^2]}, & w^* > 0 \\ 2u^{*3} [1 - hf / (\kappa u^*)] / (gh^2/\theta_v) \partial \theta_v^+ / \partial z + 7u^{*2}, & w^* = 0 \end{cases} \quad (13)$$

The expressions are meant to apply under normal conditions where the overlying air mass is stable or neutral ($\partial \theta_v^+ / \partial z \geq 0$). The effect of increasing tropospheric stability is to retard the growth of the PBL by turbulent entrainment.

In addition to the physical boundary layer height h , at least six independent length scales can be defined from the boundary conditions, physical constants and properties of the large-scale flow:

$$\left. \begin{aligned} z_0 &\equiv z |_{\bar{u} \rightarrow 0} \\ L &\equiv \theta_{vs} u^{*2} / (\kappa g \theta_v^*) \\ &= -C_D^{\frac{1}{2}} C_H^{-1} U_h^2 \theta_{vh} [\kappa g (\theta_{vs} - \theta_{vh})]^{-1} \\ h_e &\equiv \kappa u^* / f = C_D^{\frac{1}{2}} \kappa U_h f^{-1} \\ x_\theta &\equiv [u^{*2} / (gh)] (\partial \ln \langle \theta_v \rangle / \partial x)^{-1} \\ &= C_D U_h^2 (gh \partial \ln \langle \theta_v \rangle / \partial x)^{-1} \\ y_\theta &\equiv [u^{*2} / (gh)] (\partial \ln \langle \theta_v \rangle / \partial y)^{-1} \\ &= C_D U_h^2 (gh \partial \ln \langle \theta_v \rangle / \partial y)^{-1} \\ z_\theta &\equiv [u^{*2} / (gh)] (\partial \ln \theta_v^+ / \partial z)^{-1} \\ &= C_D \cdot U_h^2 (gh \partial \ln \theta_v^+ / \partial z)^{-1} \end{aligned} \right\} \quad (14)$$

These are the surface aerodynamic roughness z_0 (an empirical property of the underlying terrain over land), the Monin-Obukhov (1953) surface buoyancy length L , the Coriolis parameter length scale h_c , length scales for large-scale thermal gradients in PBL coordinates x_θ and y_θ , and a length scale for the stability of the air above z_θ . Inclusion of von Kármán's constant $\kappa \approx 0.35$ in L and h_c is traditional (Zilitinkevich, 1975a). Note that h approaches a constant value near h_c rigorously in neutral "Ekman layers" only when boundary conditions are constant over time scales of $1/f$ or more, although Clarke's (1970) data averaged over many near-neutral conditions suggest $h \approx (1/3)u^*/f \approx h_c$ may be a good approximation for average neutral data.

Now, with the physical boundary layer height h known, say from the solution of (6) using the entrainment rates of (13), the foregoing considerations suggest a parameterization of C_D , C_H , Ψ_h , etc., in terms of the local values of h/z_0 , h/L , h/h_c , h/x_θ , h/y_θ and h/z_θ —the bulk similarity parameters for surface roughness, PBL stability, Coriolis effects, baroclinicity and stability of the overlying air, respectively. For such "local similarity" to hold, we shall require that the normalized dependent variables and ancillary quantities

$$\left. \begin{aligned} \hat{u} &\equiv \kappa \bar{u}/u^*, & \hat{v} &\equiv \kappa \bar{v}/u^*, & \hat{\theta}_v &\equiv \kappa(\bar{\theta}_v - \theta_{v\theta})/\theta_v^* \\ \hat{\tau}_x &\equiv \tau_x/(\rho u^{*2}), & \hat{\tau}_y &\equiv \tau_y/(\rho u^{*2}), & & \\ \hat{F}_b &\equiv -F_b/(\rho C_p u^* \theta_v^*) & & & & \\ \hat{K}_m &\equiv K_m/(\kappa h u^*), & \hat{K}_h &\equiv K_h/(\kappa h u^*), & \hat{l}_N &\equiv l_N/h \\ \hat{u}_\theta &\equiv \kappa u_\theta/u^*, & \hat{v}_\theta &\equiv \kappa v_\theta/u^*, & \hat{w}_e &\equiv w_e/(\kappa u^*) \end{aligned} \right\} (15)$$

be functions at most of the *similarity independent variable*

$$\eta(z,t) \equiv z/h(t) \quad (16)$$

and the bulk parameters h/z_0 , h/L , etc. That is, they do not depend on the t coordinate explicitly. Implicitly, of course, a time and/or location dependence is implied through the local values of the slowly evolving bulk parameters.

A key step in obtaining the similarity equations is transforming the $d(\)/dt$ and $\partial(\)/\partial z$ operators in the governing equations to forms involving only derivatives with respect to η , henceforth denoted by $(\)' \equiv d(\)/d\eta$. To do this we first form the partial derivatives of (16) $\partial\eta/\partial t|_z = -zk^{-2}dh/dt = -\eta k^{-1}dh/dt$ and $\partial\eta/\partial z|_t = k^{-1}$, and then apply the chain rule and Eqs. (5) [$dz/dt \equiv \bar{w} = w_h \eta$] and (6) [$dh/dt = w_h + w_e$] to get

$$\begin{aligned} d\eta/dt &= \partial\eta/\partial t|_z + (dz/dt)\partial\eta/\partial z|_t \\ &= -\eta k^{-1}(dh/dt - w_h) = -(w_e/h)\eta. \end{aligned}$$

Again applying the chain rule, the total time and partial vertical derivatives are

$$d(\)/dt = (d\eta/dt)\partial(\)/\partial\eta = -w_e\eta(\)'/h, \quad (17a)$$

$$\partial(\)/\partial z = \partial\eta/\partial z|_t \partial(\)/\partial\eta = (\)'/h, \quad (17b)$$

where consistent with the local similarity approxima-

tion a possible contribution from explicit time derivatives in (17a) has been dropped.

4. Similarity equations and closure functions

Applying the relations and transformations (12a)–(12c) and (14)–(17b) to Eqs. (1a)–(1f), (4a, b), (7)–(10) and (13) gives the following set of ordinary differential equations, lower boundary conditions and ancillary relations:

$$\hat{u}' = \hat{K}_m^{-1} \hat{\tau}_x, \quad \hat{u}(z_0/h) = 0, \quad (18a)$$

$$\hat{v}' = \hat{K}_m^{-1} \hat{\tau}_y, \quad \hat{v}(z_0/h) = 0, \quad (18b)$$

$$\hat{\theta}'_v = \hat{K}_H^{-1} \hat{F}_b, \quad \hat{\theta}_v(z_0/h) = 0, \quad (18c)$$

$$\hat{\tau}'_x = -\hat{w}_e \eta \hat{u}' - (h/h_c)(\hat{v} - \hat{v}_\theta), \quad \hat{\tau}_x(z_0/h) = 1, \quad (18d)$$

$$\hat{\tau}'_y = -\hat{w}_e \eta \hat{v}' + (h/h_c)(\hat{u} - \hat{u}_\theta), \quad \hat{\tau}_y(z_0/h) = 0, \quad (18e)$$

$$\hat{F}'_b = -\hat{w}_e \eta \hat{\theta}'_v, \quad \hat{F}_b(z_0/h) = 1, \quad (18f)$$

$$\hat{K}_m = \alpha^{-1} \hat{K}_H = 8.2\beta^2 \hat{l}_N^2 (\hat{u}'^2 + \hat{v}'^2)^{1/2} [1 - \alpha(1 + \gamma) \text{Ri}]^{1/2}, \quad (19)$$

$$\hat{l}_N = 0.052 [1 - \exp(-6.7\eta)], \quad (20)$$

$$\text{Ri} = (h/L) \hat{\theta}'_v (\hat{u}'^2 + \hat{v}'^2)^{-1/2}, \quad (21)$$

$$\hat{v}_\theta = -0.35 C_D^{-1/2} \sin \Psi_h + \Delta \hat{v}_h + (h_c/x_\theta)(\eta - 1), \quad (22a)$$

$$\hat{u}_\theta = +0.35 C_D^{-1/2} \cos \Psi_h + \Delta \hat{u}_h - (h_c/y_\theta)(\eta - 1), \quad (22b)$$

$$\hat{w}_e = \begin{cases} \frac{15(-h/L)\{1 + 0.4(-h/L)^{-1}[1 - (h/h_c)]\}}{(h/z_0) + 18(-h/L)^{1/2}[1 + 0.4(-h/L)^{-1}]}, & h/L < 0 \\ 6[1 - (h/h_c)] / (h/z_0) + 7, & h/L = 0 \end{cases} \quad (23)$$

where the caret denotes a dimensionless transformed dependent variable or ancillary quantity defined in (15).

To close the similarity formulation we need to specify α , β and γ appearing in the eddy diffusivity expressions (19). It is shown in Appendix B that near the surface ($z_0/h \leq \eta \ll 1$) the closure functions take the form

$$\left. \begin{aligned} \alpha(\zeta) &= \phi_m \phi_H^{-1} \\ \beta(\zeta) &= \phi_m^{-1} \phi_\epsilon^{-1} \\ \gamma(\zeta) &= -1 + (\phi_m - \phi_\epsilon) \zeta^{-1} \end{aligned} \right\}, \quad (24)$$

where $\zeta = z/L$ is the *surface layer* stability variable and

$$\left. \begin{aligned} \phi_m(\zeta) &\equiv \frac{\kappa z}{u^*} \frac{\partial \bar{u}}{\partial z} = \begin{cases} (1 - 15\zeta)^{-1/2}, & \zeta < 0 \\ 1 + 4.7\zeta, & \zeta \geq 0 \end{cases} \\ \phi_H(\zeta) &\equiv \frac{\kappa z}{\theta_v^*} \frac{\partial \bar{\theta}_v}{\partial z} = \begin{cases} 0.74(1 - 9\zeta)^{-1/2}, & \zeta < 0 \\ 0.74 + 4.7\zeta, & \zeta \geq 0 \end{cases} \\ \phi_\epsilon(\zeta) &\equiv \frac{\kappa z \epsilon}{u^{*3}} = \begin{cases} (1 + 0.5|\zeta|^{1/2})^{1/2}, & \zeta < 0 \\ (1 + 2.5\zeta^2)^{1/2}, & \zeta \geq 0 \end{cases} \end{aligned} \right\} \quad (25)$$

are the Monin-Obukhov surface layer similarity functions for shear, buoyancy flux and dissipation. The expressions given in (25) were derived by Businger *et al.* (1971) and Wyngaard and Coté (1971) from curve fits to meteorological tower data. Note the different functional forms for unstable ($\zeta < 0$) and stable ($\zeta > 0$) conditions and that $\phi_m, \phi_\epsilon \rightarrow 1, \phi_H \rightarrow 0.74$ as $\zeta \rightarrow 0$. Clearly, α, β and γ are not constants near the surface but relate uniquely to ϕ_m, ϕ_H and ϕ_ϵ and therefore to the relative location and the stability.

On the other hand, the surface layer forms of the closure functions are unlikely to apply unmodified in the upper regions where turbulence characteristics are different. To extend the closure functions to these upper regions we hypothesize that since the turbulence property which differs most obviously in behavior above the surface layer is the mixing length (approaching a constant fraction of the height rather than varying linearly with distance from the surface), we may apply Eqs. (24) and (25) for $\alpha(\zeta), \beta(\zeta)$ and $\gamma(\zeta)$ anywhere in the boundary layer provided we redefine the argument of these functions as proportional to the ratio of the local neutral mixing length to the Monin-Obukhov length, i.e.,

$$\zeta \equiv l_N / (\kappa L).$$

Again it proves useful to incorporate von Kármán's constant since the neutral mixing length has the form $l_N = \kappa z$ near the surface, so the proper form of the surface layer stability variable z/L is recovered automatically. Above, ζ is compressed consistent with the observed variation of the turbulent mixing length away from a solid boundary.

Using (20) to express the variation of the normalized neutral mixing length through the boundary layer we may now write the argument of the closure functions as

$$\zeta(\eta, h/L) = \kappa^{-1} (h/L) l_N^2 = 0.15 (h/L) [1 - \exp(-6.7\eta)]. \quad (26)$$

This implies the closure functions, too, are functions of relative position with the overall bulk stability as a parameter: $\alpha = \alpha(\eta, h/L), \beta = \beta(\eta, h/L), \gamma = \gamma(\eta, h/L)$. Fig. 1a shows $\alpha(\zeta), \beta(\zeta), \gamma(\zeta)$ computed from (24) and (25); in Fig. 1b are contours of $\eta(\zeta)$ from (26) for various h/L 's. Together these give α, β and γ for any η between z_0/h and 1 for the indicated values of the bulk stability parameter. Notice that the diffusivity ratio $\alpha \equiv K_H/K_m$ varies markedly on the unstable side favoring sensible heat (and buoyancy) diffusion as $\zeta \rightarrow -\infty$. The buoyant/neutral mixing length ratio $\beta = l_N/l$ increases for unstable flows but drops off sharply on the stable side. Note the sign change in the "transport"/buoyancy-flux ratio γ at $\zeta \approx -1.95$ and again at the $\zeta = 0$ singularity. Fortunately, the singularity in γ at neutral stability does not lead to problems since an analysis will verify the term $\alpha(1+\gamma) Ri$ in Eqs. (9) and (19) goes to zero as $\zeta \rightarrow 0$ and the proper form of the Prandtl mixing length theory in the neutral

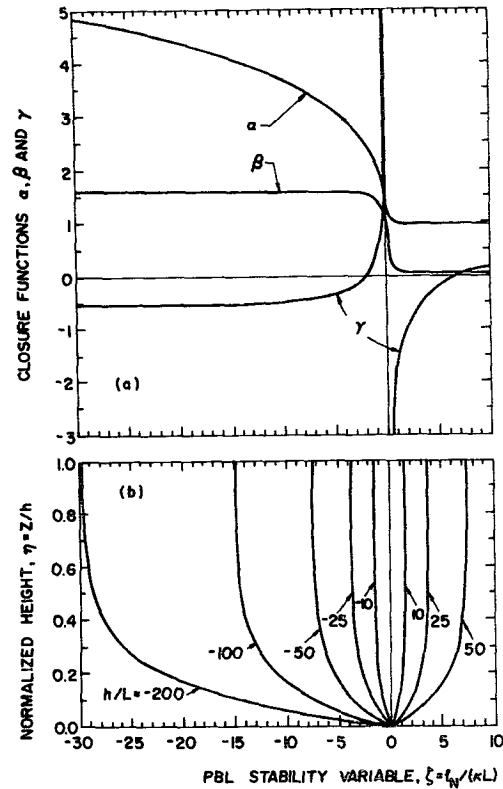


FIG. 1. Closure functions (a) and similarity height coordinate η (b) as a function of ζ computed from Eqs. (24) and (25) in (a) and Eq. (26) in (b). Such curves effectively define $\alpha(\eta; h/L), \beta(\eta; h/L)$ and $\gamma(\eta; h/L)$ anywhere in the boundary layer.

limit is recovered. (In the same limit γ goes to plus or minus infinity depending on whether $\zeta = 0$ is approached from the unstable or stable side, respectively.) Thus, the present formulation of the closure functions insures Monin-Obukhov similarity near the surface and is consistent with traditional mixing-length theory for the neutral case. Under buoyantly interactive conditions the formulation for the upper boundary layer is plausible, but must still be validated against appropriate experiments.

Having closed the system of similarity equations mathematically, we now consider some properties of the system and problems associated with numerical solution. Suppose that we have specified the bulk parameters $h/z_0, h/L, h/h_c, h/x_0, h/y_0$ and h/z_0 , and have some way of specifying the self-consistent values of $C_D, \Psi_h, \Delta u_h$ and $\Delta \theta_h$ appearing in the geostrophic wind relations (22a, b). We could then integrate (18a)–(18f) numerically, applying (19)–(26) locally at each step¹ from the initial surface point $\eta_0 = z_0/h$ to any point η in the

¹ We find it helps to start such integrations with surface-layer-consistent derivatives in (19) and (21):

$$u'(\eta_0) = \phi_m(\zeta_0)\eta_0^{-1} \approx h/z_0, \quad v'(\eta_0) = 0, \\ \theta'_v(\eta_0) = \phi_H(\zeta_0)\eta_0^{-1} \approx 0.74h/z_0,$$

where the approximations apply because $\zeta_0 = z_0/L \ll 1$.

boundary layer to find the similarity profiles $\hat{u}(\eta)$, $\hat{v}(\eta)$, $\hat{\theta}_v(\eta)$, $\hat{\tau}_x(\eta)$, $\hat{\tau}_y(\eta)$ and $\hat{F}_b(\eta)$. At $\eta = \eta_h$ the solutions will have attained some finite edge values \hat{u}_h , \hat{v}_h , $\hat{\theta}_{vh}$, $\hat{\tau}_{xh}$, $\hat{\tau}_{yh}$ and \hat{F}_{bh} . From their definitions we may write the drag and heat transfer coefficients and the internal turning angle in terms of normalized edge quantities:

$$C_D = \kappa^2(\hat{u}_h^2 + \hat{v}_h^2)^{-1}, \quad C_H = \kappa^2(\hat{u}_h^2 + \hat{v}_h^2)^{-1/2} \hat{\theta}_{vh}^{-1}, \quad (27)$$

$$\Psi_h = \tan^{-1}(-\hat{v}_h/\hat{u}_h). \quad (28)$$

Had we chosen C_D and Ψ_h consistently, the drag coefficient and turning angle computed from the normalized edge velocities at the end of the integration using the above relations would agree with those chosen initially. Alternately, we can view the initial choice as the first step in an iterative sequence in which successive integrations of (18a)–(18f) are performed with new C_D and Ψ_h values until these compatibility conditions are satisfied by the numerical solutions to within some small error bound.

In the presence of edge discontinuities, additional iterative loops may be needed since $\Delta\hat{u}$ and $\Delta\hat{v}$ are initially unknown functions of the bulk parameters as well. We consider first the “classical” boundary layer problem where upper boundary conditions on velocity and temperature are applied at $\eta \rightarrow \infty$ (Schlichting, 1960; Zilitinkevich, 1970, 1975a). For this case the mere boundedness of \hat{u} , \hat{v} and $\hat{\theta}_v$ at infinity insures that vertical derivatives at the edge vanish (\hat{u}' , \hat{v}' , $\hat{\theta}'_v = 0$ as $\eta \rightarrow \infty$). Since the effective diffusivity of air (eddy diffusivity plus molecular diffusivity) is always finite, Eqs. (18a, b, c) then imply vanishing Reynolds stress and buoyancy flux at the edge ($\hat{\tau}_x$, $\hat{\tau}_y$, $\hat{F}_b = 0$ as $\eta \rightarrow \infty$). Note that vanishing turbulent fluxes at the upper boundary in the classical case are *not*, properly speaking, boundary conditions, but consequences of the boundedness of velocity and temperature at infinity.

We now consider the case of interest here with the boundary layer height defined at a finite height $z = h$ ($\eta = 1$), where an idealized discontinuity or jump³ in properties may have to be introduced to get the fluxes to vanish above. Physically, such discontinuities may represent capping inversion lids—local buoyantly stable zones ($\partial\hat{\theta}_v/\partial z$, $-F_b > 0$) at the top of well-mixed convective PBL's which suppress boundary layer turbulence and define the moving upper boundary $h(t)$. Below such discontinuities the generally finite edge fluxes are given by the integrals of (18d, e, f):

$$\hat{\tau}_{xh} = 1 + \int_{\eta_0}^1 \hat{\tau}'_x d\eta, \quad \hat{\tau}_{yh} = \int_{\eta_0}^1 \hat{\tau}'_y d\eta, \quad \hat{F}_{bh} = 1 + \int_{\eta_0}^1 \hat{F}'_b d\eta.$$

Imposing a zero turbulence condition *above* the discontinuity, we can find the corresponding jumps in velocity and temperature by integrating both sides of

(18d, e, f) across a “thin” slab centered at $\eta = 1$:

$$\left. \begin{aligned} \Delta\hat{u}_h &\equiv \hat{u}_h^+ - \hat{u}_h = \hat{\tau}_{xh}/\hat{w}_e, & \Delta\hat{v}_h &\equiv \hat{v}_h^+ - \hat{v}_h = \hat{\tau}_{yh}/\hat{w}_e \\ \Delta\hat{\theta}_{vh} &\equiv \hat{\theta}_{vh}^+ - \hat{\theta}_{vh} = \hat{F}_{bh}/\hat{w}_e \end{aligned} \right\}. \quad (29)$$

These jumps are effectively identical to those derived by Lilly (1968), Tennekes (1973), Deardorff (1973) and Mahrt and Lenschow (1976) for an infinitesimally thick inversion lid.

In practice, the nonturbulent regions above PBL inversion layers are often vertically nonuniform with gradients of velocity and virtual potential temperature which affect the structure of the upper PBL, particularly the inversion layer. We now consider a slight modification of the similarity formulation which accounts for such “gradients at infinity”, treating only the influence of a finite stable lapse rate above $\partial\theta_v^+/\partial z$ at this point, but recognizing that extensions to flows with finite ($\partial u^+/\partial z$, $\partial v^+/\partial z$) are also possible and fairly straightforward.

A fundamental principle of similarity-transforming partial to ordinary differential equations is to choose dependent variable transformations which also recover the relevant boundary conditions. In the present instance, we seek a variant of the dimensionless thermal variable $\hat{\theta}_v(\eta) = \kappa(\theta_v - \theta_{vs})/\theta_v^*$ such that $\hat{\theta}_v$ is bounded at infinity ($\hat{\theta}'_v = 0$ as $\eta \rightarrow \infty$) as the physical slope $\partial\theta_v/\partial z$ approaches $\partial\theta_v^+/\partial z$. A transformation with this property is

$$\hat{\theta}_v(\eta) \equiv \kappa[\bar{\theta}_v - \theta_{vs} - (z - z_0)\partial\theta_v^+/\partial z]/\theta_v^*,$$

which reduces to the form in (15) when $\partial\theta_v^+/\partial z = 0$. Rearranging and assuming $\partial\theta_v^+/\partial z$ is a constant gives physical virtual potential temperature derivatives of the similarity form [cf. (17a, b)] $d\hat{\theta}_v/dt = (\theta_v^*/\kappa)d\hat{\theta}/dt = -[w_e\theta_v^*/(\kappa h)]\eta\hat{\theta}'_v$ and

$$\begin{aligned} \partial\hat{\theta}_v/\partial z &= [\theta_v^*/(\kappa h)][\hat{\theta}'_v + (\kappa h/\theta_v^*)\partial\theta_v^+/\partial z] \\ &= [\theta_v^*/(\kappa h)][\hat{\theta}'_v + \kappa^2(L/z_0)]. \end{aligned}$$

When the stability of the overlying air mass is accounted for in this way, Eq. (18d) is unchanged, but (18c) and (21) are modified with $\hat{\theta}'_v + \kappa^2(L/z_0)$ replacing $\hat{\theta}'_v$. In particular, the normalized buoyancy flux Eq. (18c) becomes

$$\hat{F}_b = \hat{K}_H[\hat{\theta}'_v + \kappa^2(L/z_0)],$$

where $\kappa^2(L/z_0) < 0$ for convective PBL's with stable layers above. The desirable properties $\hat{\theta}_v(z_0/h) = 0$ and $\hat{\theta}'_v(\infty) = 0$ (the limit as $\partial\hat{\theta}_v/\partial z \rightarrow \partial\theta_v^+/\partial z$) can thus be retained relatively easily in the similarity formulation when $\partial\theta_v^+/\partial z \neq 0$.

To summarize, the present similarity formulation indicates the profiles $\hat{u}(\eta)$, $\hat{v}(\eta)$, $\hat{\theta}_v(\eta)$, $\hat{\tau}_x(\eta)$, $\hat{\tau}_y(\eta)$, $\hat{F}_b(\eta)$ as well as C_D , C_H , Ψ_h , $\Delta\hat{u}_h$, $\Delta\hat{v}_h$, $\Delta\hat{\theta}_{vh}$ depend, in general, on six dimensionless parameters: h/z_0 , h/L , h/h_c , h/x_0 , h/y_0 , h/z_0 . For the general case, and treating inversion layers as discontinuities, numerical integration of (18a)–(18f) is required, with (19)–(26) applied

locally. In the present initial-value formulation a four-fold iteration for the initially unknown values of C_D , Ψ_h , $\Delta\hat{u}_h$, $\Delta\hat{v}_h$ appearing in (22a, b) using the compatibility relations (27)–(29) is needed.

In view of the many parameters and the fourfold iteration associated with the general case, we sought some reasonable approximations to the full system to test the integration and iteration schemes, and the realism of the closure model against field observations and laboratory experiments. Perhaps the simplest approximations of this type involve *ad hoc* specification of the stress and buoyancy flux profiles in some analytic form, e.g., linear, parabolic, etc. Linear profiles can be rationalized somewhat more formally by ignoring internal rotation and replacing the righthand sides of the left-hand column (18d, e, f) by constant depth-averaged values (Lilly, 1968; Csanady, 1974). Assuming further that turbulent fluxes vanish at the edge ($\hat{\tau}_{xh}$, $\hat{\tau}_{yh}$, $\hat{F}_{bh}=0$) leads to what we will call the *linear flux model*:

$$\hat{\tau}'_x = -1 \rightarrow \hat{\tau}_x(\eta) = 1 - \eta, \tag{18d'}$$

$$\hat{\tau}'_y = 0 \rightarrow \hat{\tau}_y(\eta) = 0, \tag{18e'}$$

$$\hat{F}'_b = -1 \rightarrow \hat{F}_b(\eta) = 1 - \eta. \tag{18f'}$$

Computationally, replacing (18d)–(18f) by these approximate profiles has the effects of eliminating any need for iteration. The similarity equations for the *linear shear layer* problem are straightforward integrations from initial values in two parameters, h/z_0 and h/L . Physically, the approximation may be justified where the major effects are roughness and buoyancy, e.g., wind tunnel boundary layers with strong surface heating or cooling. Csanady (1974) makes a similar approximation to analyze the barotropic PBL with negligible turning below an inversion lid. Under baroclinic conditions the detailed computations of Wyinggaard and Coté (1974) show stress profiles which are more nearly parabolic.²

However, approximations based on depth-averaging (18d, e) cannot properly account for internal turning Ψ_h driven by the depth-dependent geostrophic departure ($\hat{u}-\hat{u}_g$, $\hat{v}-\hat{v}_g$). To check the turning calculation we used the *quasi-steady Ekman model*:

$$\hat{\tau}'_x = -(h/h_c)(\hat{v} + 0.35C_D^{-1/2} \sin\Psi_h), \tag{18d''}$$

$$\hat{\tau}'_y = +(h/h_c)(\hat{u} - 0.35C_D^{-1/2} \cos\Psi_h), \tag{18e''}$$

$$\hat{F}'_b = -1. \tag{18f''}$$

This can be derived from the full similarity formulation

² Parabolic stress profiles are also obtained from the present model under baroclinic conditions by retaining the linear variation of the geostrophic winds in (22a,b), depth-averaging the other terms in (18d,e,f) and integrating:

$$\begin{aligned} \hat{\tau}_x(\eta) &= 1 + [\hat{\tau}_{xh} - 1 - (\frac{1}{2})(h/x_g)]\eta + (\frac{1}{2})(h/x_g)\eta^2, \\ \hat{\tau}_y(\eta) &= [\hat{\tau}_{yh} - (\frac{1}{2})(h/y_g)]\eta + (\frac{1}{2})(h/y_g)\eta^2, \\ \hat{F}_b(\eta) &= 1 + (\hat{F}_{bh} - 1)\eta. \end{aligned}$$

by neglecting the entrainment terms compared with the geostrophic departure terms in (18d, e) and assuming a constant (barotropic) geostrophic wind and negligible edge velocity jumps in (22a, b). Strictly speaking the quasi-steady Ekman model applies only to the stationary nonentraining neutral PBL with upper boundary conditions at infinity such as that studied by Blackadar (1962). We have, however, extended the model as an approximation to buoyantly interactive cases as well where we retain the simple flux gradient of the linear model. Computationally the quasi-steady Ekman model requires specification of three bulk parameters h/z_0 , h/L and h/h_c , and involves a double iteration on C_D and Ψ_h after each trial integration until convergence.

To implement these approximations we developed computer codes for solving the linear flux model and the quasi-steady Ekman models on the IBM 360/95 at the Goddard Institute for Space Studies. A predictor-corrector scheme was used for upward integration through the boundary layer with a variable step size chosen by the program to give uniform accuracy as the computation progressed through regions of large gradient (the surface layer) to upper regions where the gradient becomes much less steep and larger steps are appropriate. The iterations on C_D and Ψ_h needed for the quasi-steady Ekman model are done by establishing linear relaxation factors from trial calculations and varying the drag coefficient and turning angle to reduce the difference between the guessed values and values computed from (27) and (28) at the end of each integration. Convergence is generally obtained after four to ten integrations, a few seconds or less on the IBM 360/95.

5. Comparison with observations

As initial tests of the similarity model we compared the boundary layer structures computed from the foregoing approximations with selected field observations and laboratory experiments.

We sought first to determine whether the turbulence closure hypothesis used with the quasi-steady Ekman model would give a reasonably good description of the influence of buoyant stability on PBL structure, internal turning, drag coefficients, etc. For this purpose the balloon measurements by Clarke (1970) during the Kerang and Hay field trials in Australia seemed representative of PBL observations over a wide range of stability conditions [see also the discussion of this data by Sheppard (1970)]. Clarke has subsumed his PBL profile data into four stability classes whose average properties in terms of similarity model parameters are given in Table 1. Here we interpreted Clarke's dimensionless roughness \hat{z}_0 as $\kappa z_0/h_c$ and his stability parameter sk^2 as h_c/L . We determined h/h_c from estimated class-mean inversion lid heights for the unstable classes (I and II) and from Deardorff's interpolation

TABLE 1. Model parameters for Clarke's (1970) measurements of vertical flow profiles in the planetary boundary layer.

Parameters	Stability class			
	I Very un- stable	II Unstable	III Near-neutral	IV Stable
h/z_0	2.4×10^5	1.2×10^5	3.4×10^5	5.9×10^3
h/L	-140	-33	0	+22
h/h_c	1.00	0.40	1.00	0.26

formula $h/h_c = [1 + h_c/(30L)]^{-1}$ for the stable class IV [Zilitinkevich (1972) suggests a correlation of the form $h/h_c \propto (h_c/L)^{-1/2}$ when $h_c/L \gg 1$, but such correlations are likely to be ineffective in data analysis when entrainment and other unsteady effects are present]. This gave $h/z_0 = (\kappa z_0)(h/h_c)$ and $h/L = s\kappa^2(h/h_c)$, except for class III modeled as strictly neutral.

The similarity profiles $\hat{u}(\eta)$, $\hat{v}(\eta)$ and $\hat{\theta}_v(\eta)$ computed with the quasi-steady Ekman model for stability classes I, II, and III using the Table 1 bulk parameters are compared with Clarke's class-averaged measurements in Fig. 2. For these unstable and neutral cases

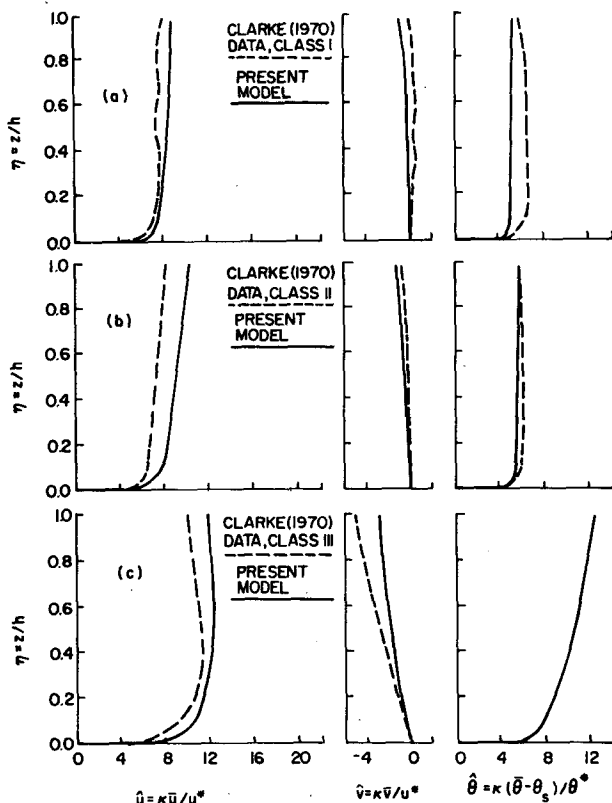


FIG. 2. Dimensionless mean wind component and potential temperature profiles. Similarity solutions of the quasi-steady Ekman model are compared with Clarke's (1970) observations for the (a) very unstable, (b) unstable and (c) near-neutral stability classes using the bulk parameters of Table 1.

this approximation to the full similarity model gave a reasonably good description of the profile data including a qualitatively correct picture of internal rotation of the horizontal velocity vector. However, some of the detailed structural features of inversion-capped convective PBLs are left out because the quasi-steady Ekman model doesn't consistently account for the edge discontinuities generated at finite-height entrainment surfaces.

For example, the potential temperature profiles in Clarke's unstable classes exhibit slope reversals near the edge which are not exhibited by the model solutions $[(\hat{\theta}')_h < 0$ in the data whereas the model gives $\hat{\theta}' \geq 0$ everywhere—see also the original plots in Fig. 1 of Clarke (1970)]. These elevated stable zones are apparently finite-width inversion lids which are further spread out by averaging over the many realizations. Notice however that negative $\hat{\theta}_v$ gradients near the edge give $\hat{F}_{bh} < 0$ from (18c) associated physically with entrainment of negative buoyancy through the capping inversion. Deardorff (1972) suggests parameterization of the surface-flux-normalized, inversion-base buoyancy flux as a negative constant $\hat{F}_{bh} \approx -0.2$ for strongly convective conditions, although we have assumed $\hat{F}_{bh} = 0$ in (18f''). We do this as a simplification and because Lenschow's (1974) observations indicate values closer to zero in the -0.1 to -0.05 range, while the detailed calculations by Zeman (1975) show a marked variation of \hat{F}_{bh} with the bulk stability parameter h/L . The variation of \hat{F}_{bh} with the bulk parameters h/L , h/h_c , etc., is given in principle by the full formulation of the similarity model.

On the other hand, the edge Reynolds stresses computed with the quasi-steady Ekman model can depart appreciably from zero, particularly in the unstable cases, as shown in the $\hat{\tau}_x(\eta)$ and $\hat{\tau}_y(\eta)$ profiles computed with the Table 1 parameters and plotted in Fig. 3. The possibility of finite edge stresses was discussed earlier in connection with upper boundary conditions imposed at a finite height as opposed to infinity. In the full similarity formulation the velocity (\hat{u}, \hat{v}) would jump to geostrophic conditions and $(\hat{\tau}_x, \hat{\tau}_y)$ would jump to zero just above $\eta = 1$; but by neglecting $(\Delta \hat{u}_h, \Delta \hat{v}_h)$ in (22a, b) and the associated entrainment terms in (18d, e) in the quasi-steady Ekman model, we have introduced a potential source of error in the stress profiles near the edge, as well as an inconsistency³

³ Little is known observationally of inversion-base Reynolds stresses, but following Zeman's (1975) approximate analysis of convective PBL's we can make some estimates: He assumes a well mixed layer ($\hat{u} \approx \hat{u}_0$; \hat{u}' , $\Delta \hat{u}_h \approx 0$) with no internal rotation ($\hat{v}, \hat{v}', \Psi_h \approx 0$) but with a normal velocity component induced above the upper boundary jump ($\Delta \hat{v}_h \approx \hat{v}_h^+ \approx \hat{v}_0$). Under these conditions (18d) gives $\hat{\tau}_x \approx (h/h_c) \Delta \hat{v}_h$ and (29) gives

$$\hat{\tau}_{zh} = 1 + \int_{\eta_0}^1 \hat{\tau}'_x d\eta = 1 + (h/h_c) \Delta \hat{v}_h = \hat{v}_0 \Delta \hat{u}_h \approx 0.$$

Accordingly, $\Delta \hat{v}_h \approx -h_c/h$, so the normal edge stress component

between the zero \hat{F}_{bh} and finite $\hat{\tau}_{xh}$ and $\hat{\tau}_{yh}$. Nonetheless, the model does recover the neutral limit of Blackadar (1962), and despite missing the inversion-lid details in the unstable case, gives eddy diffusivity profiles $\hat{K}_m(\eta)$ for classes I, II and III shown in Fig. 3 which are plausible and qualitatively correct. Some caution is appropriate in interpreting Clarke's (1970) "observational" curves for stress and diffusivity as these are not direct measurements but quantities derived from the geostrophic departures and their integrals.

Although numerical integration of the quasi-steady Ekman model was straightforward with the unstable and neutral classes of Table 1, we were not able to get a converged solution for Clarke's stable class IV. The inability of the computer code to find a solution to the stable case apparently stems from the fact that the middle part of the boundary layer was nonturbulent, consistent with Businger's (1973) picture of the unsteady stable layer which forms during the diurnal cycle, indicating that a continuous, turbulently linked structure may not exist for these bulk parameters. This conclusion is supported by Clarke's estimate that the critical Richardson number ($Ri_{cr} \approx 0.2$) was exceeded above the first 10% of h_c in class IV leading to a nonsteady laminar behavior he calls "undulance".

In view of the problems associated with entraining inversion lids, Coriolis effects and nonturbulent regimes in stable layers, we sought a validation for the closure model in which these effects were absent and where the dominant effects on the boundary layer profiles and exchange coefficients were surface roughness and buoyancy. These conditions have been created and studied in the laboratory by Arya (1975) by thermally forcing the turbulent boundary layer formed over the floor of a wind tunnel test section. The analogy between such flows and PBL's formed in the atmosphere has not been fully explored, but minimum scaling requirements include a bulk Reynolds number $Re_h = U_h h / \nu$ large enough to get a turbulent boundary layer, and the ability to generate a range of bulk Richardson numbers $Ri_h = gh(\theta_h - \theta_s) / (\theta_s U_h^2)$ which overlaps a significant range of atmospheric stability variations.

Arya (1975) has reported on such experiments at Colorado State University in a wind tunnel (test section, 1.8 m x 1.8 m x 28 m), wherein a heated or cooled aluminum floor plate and an ambient-air air conditioning system were used to generate a range of turbulent, buoyantly interactive boundary layers. Mean and fluctuating velocity and temperature profiles in these layers were measured with Pitot-probe, thermocouple and hot-wire anemometer instruments with a cold-wire resistance thermometer used to correct for

from (29) is $\hat{\tau}_{yh} \approx -\hat{w}_e(h_c/h)$. Since (23) indicates \hat{w}_e can be order unity or greater when $-h/L \gg 1$, this analysis implies inversion-base stresses of order the surface stress under strongly convective conditions.

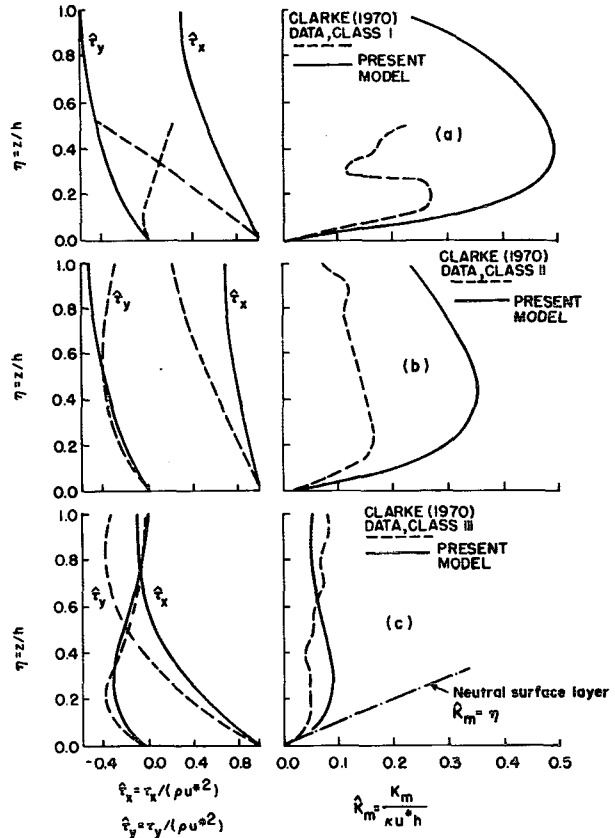


FIG. 3. As in Fig. 2 except for the dimensionless Reynolds stress component and momentum eddy diffusivity profiles.

temperature fluctuation effects. Boundary layer thicknesses h in these experiments were roughly 0.5 m [$(h/h_c) \sim 0.5 \times 10^{-3}$]. Reynolds numbers in the turbulent range ($Re_h \sim 10^6$) were obtained by driving the flow with boundary layer edge velocities U_h in the range of 3–9 m s⁻¹, comparable to atmospheric wind speeds at the PBL edge. Accordingly, the bulk Richardson number was controlled essentially by manipulating the $h \times \Delta\theta$ product. Thus to compensate for the small (compared to atmospheric) boundary layer thickness h rather large temperature differences across the layer were used, $\Delta\theta = \theta_h - \theta_s \approx -150$ K in the most unstable runs. Table 2 gives the measured values of U_h/u_*^* , $(\theta_h - \theta_s)/\theta_s^*$ and h/L for six stability classes used by Arya. [The definition of stability classes in Table 2 and some of the numerical values differ somewhat from those in Arya (1975) but are consistent with an earlier preprint of the work from which we derived them. The variations between these sets of numbers is real but small and does not materially change the results presented here.] The roughness height z_0 was not tabulated or otherwise cited by Arya, so we estimated a constant value of h/z_0 by fitting the drag data.

Since the primary factors shaping the profiles in these experiments were roughness and buoyancy we used the linear flux model approximation to compare with the

TABLE 2. Model parameters for Arya's measurements of turbulent, thermally stratified wind-tunnel boundary layers.

Parameter	Stability class					
	VI	V	IV	I	II	III
h/z_0	1.7×10^3					
h/L	-3.2	-1.6	-1.0	+0.1	+0.3	+1.4
g/h_c	0.0	0.0	0.0	0.0	0.0	0.0
U_h/u^*	19.6	22.2	24.4	28.6	32.3	41.7
$(\theta_h - \theta_s)/\theta^*$	12.5	13.7	14.9	33.3	41.7	52.6

data. Fig. 4 compares the observed velocity and temperature defect profiles with the linear flux model profiles using the Table 2 parameters. To get these curves we computed the theoretical defect profiles from the similarity variables using

$$\begin{aligned} (U_h - \bar{u})/u^* &= C_D^{-1/2} - \kappa^{-1} \hat{u}(\eta), \\ (\theta_h - \bar{\theta})/\theta^* &= C_D^{1/2} C_H^{-1} - \kappa^{-1} \hat{\theta}(\eta). \end{aligned}$$

Shown in Fig. 5 are the bulk Richardson number and drag coefficient variations computed with the linear flux model as a function of the bulk stability parameter h/L with h/z_0 held constant at 1.7×10^3 . Also shown are the wind-tunnel values computed from the Table 2

data using

$$\begin{aligned} C_D &= (U_h/u^*)^{-2}, \quad C_H = (U_h/u^*)^{-1} [(\theta_h - \theta_s)/\theta^*]^{-1}, \\ \text{Ri}_h &= \kappa^{-1} C_D^{1/2} C_H^{-1} (h/L). \end{aligned}$$

Figs. 4 and 5 indicate qualitative agreement between the linear shear layer predicted boundary layer behavior and Arya's wind tunnel data. Particularly encouraging is the fact that the similarity behavior of the aerodynamic exchange coefficients in Fig. 5 was properly predicted for the stable as well as the unstable classes.

As a final test of the approximate formulations we looked at the quasi-steady Ekman model's prediction of individual terms in the turbulent kinetic energy

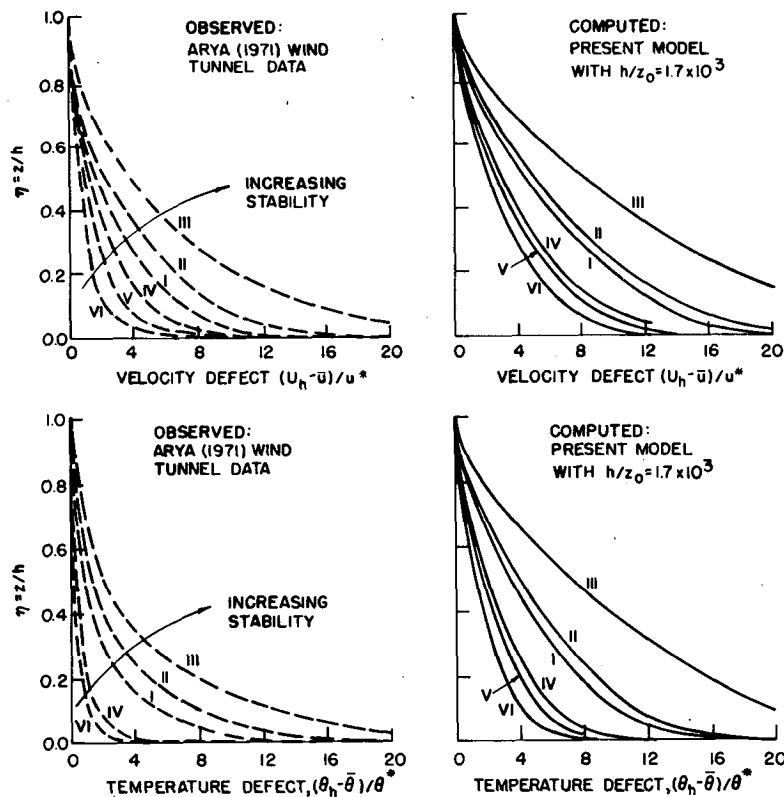


FIG. 4. Velocity defect and temperature defect profiles. Similarity solutions of the linear flux model are compared with Arya's (1975) data for thermally-stratified boundary layers in a wind tunnel using the bulk parameters of Table 2.

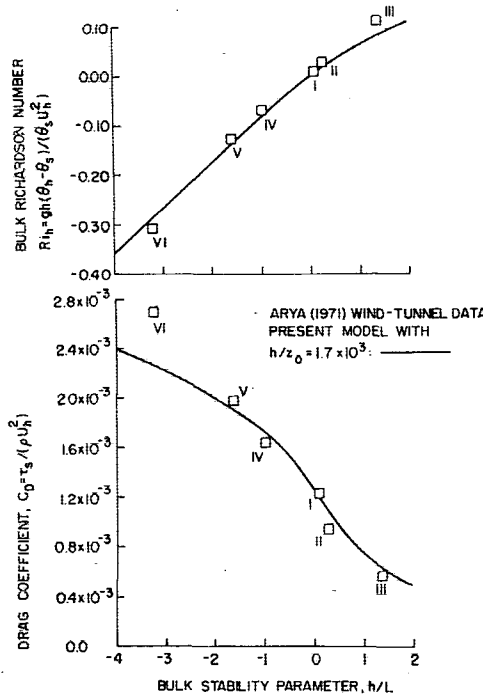


Fig. 5. Richardson number and drag coefficient as a function of the bulk stability parameter. Coefficient variations computed from similarity solutions of the linear flux model are compared with Arya's (1975) data for thermally-stratified boundary layers in a wind tunnel using the bulk parameters of Table 2.

balance throughout the PBL in comparison with Lenschow's (1974) aircraft field measurements under convective conditions. Three sets of observations were compared corresponding to the conditions of Table 3. For each set Lenschow plots the vertical profile of "transport", shear production, buoyant production and dissipation components of the turbulent kinetic energy balance [Eq. (2)] normalized by the value of buoyancy flux at the surface. In terms of the present similarity variables we may write these terms as

$$Tr(\eta) \equiv \frac{-\partial G / \partial z - \rho d\bar{e} / dt}{gF_{bs} / (C_p \theta_v)} = \gamma(\eta) \hat{F}_b(\eta), \quad (30a)$$

$$S(\eta) \equiv \frac{\tau_x \partial \bar{u} / \partial z + \tau_y \partial \bar{v} / \partial z}{gF_{bs} / (C_p \theta_v)} = \frac{\hat{F}_b(\eta)}{\alpha(\eta) Ri(\eta)}, \quad (30b)$$

$$B(\eta) \equiv \frac{gF_b / (C_p \theta_v)}{gF_{bs} / (C_p \theta_v)} = \hat{F}_b(\eta), \quad (30c)$$

$$D(\eta) \equiv \frac{\rho \epsilon}{gF_{bs} / (C_p \theta_v)} = \frac{\kappa^4 \hat{K}_m^3(\eta)}{(h/L) \beta^4(\eta) \lambda_N^4(\eta)}. \quad (30d)$$

By definition these terms are in balance when $Tr + S + B - D = 0$. The fact that $\alpha(\eta)$, $\beta(\eta)$ and $\gamma(\eta)$ are uniquely related to $S(\eta)$, $D(\eta)$ and $Tr(\eta)$, respectively, makes this type of comparison particularly

useful for checking the behavior of the similarity closure functions in the upper PBL. But note that the "transport" term (30a) is itself resolvable into four components

$$Tr = -\frac{C_p \theta_v}{gF_{bs}} \left[\frac{\partial(\overline{w'e'})}{\partial z} + \frac{1}{\rho} \frac{\partial(\overline{w'p'})}{\partial z} + \frac{\partial \bar{e}}{\partial t} + \langle \mathbf{U} \rangle \cdot \nabla \bar{e} \right].$$

diffusion pressure transport unsteady effects advection effects

In many field measurements of the turbulent kinetic energy budget the "transport" term cited is the diffusion component only. Wyngaard and Coté (1971) refer to the nondiffusive parts of the transport term as an "imbalance" in the turbulent kinetic energy equation. Lenschow, too, equates the measured diffusion component with the transport term although in his 5 November 1970 experiment an additional advective component was measured and plotted. In general, however, the pressure transport and unsteady terms are difficult to measure and are left out of Lenschow's balance on grounds that the other terms' algebraic sum is near zero. This contrasts with Wyngaard and Coté's finding of an "imbalance" in the surface layer, and should be borne in mind when comparing results.

The similarity profiles of $Tr(\eta)$, $S(\eta)$, $B(\eta)$ and $-D(\eta)$ computed with the quasi-steady Ekman model using the Table 3 parameters are compared with Lenschow's (1974) data in Fig. 6. The agreement between our theory and the observed shear production, buoyant production and dissipation profiles seems acceptable, but an apparent discrepancy exists between our "transport" profile $Tr(\eta)$ and some of the Fig. 6 data insofar as our Tr becomes *positively* large near the surface. This profile differs also from the transport profile in Lenschow's (1974) turbulence budget model, which is negative near the surface, positive near the top and integrates out to zero over the PBL. The discrepancies are related to the fact that Lenschow's (1974) transport data points represent only the diffusive part of Tr , his model transport term represents diffusion and possibly pressure transport, whereas our "transport" term contains the vertical diffusion of turbulent energy plus the "imbalance" of Wyngaard and Coté (1971)—pressure transport, unsteady effects and advection. In this sense our model simply reproduces the surface layer energy balance consistent with the Monin-Obukhov functions of (25).

TABLE 3. Model parameters for Lenschow's (1974) measurements of turbulent kinetic energy budget terms in convectively unstable planetary boundary layers.

Date Location Surface	25 April 1968 Eastern Colorado Short grassland	5 November 1970 Lake Michigan Water	13 November 1970 Lake Huron Water
h/z_0	5.2×10^4	3.6×10^6	4.6×10^6
h/L	-32	-7.8	-38
h/h_c	0.60	0.57	0.99

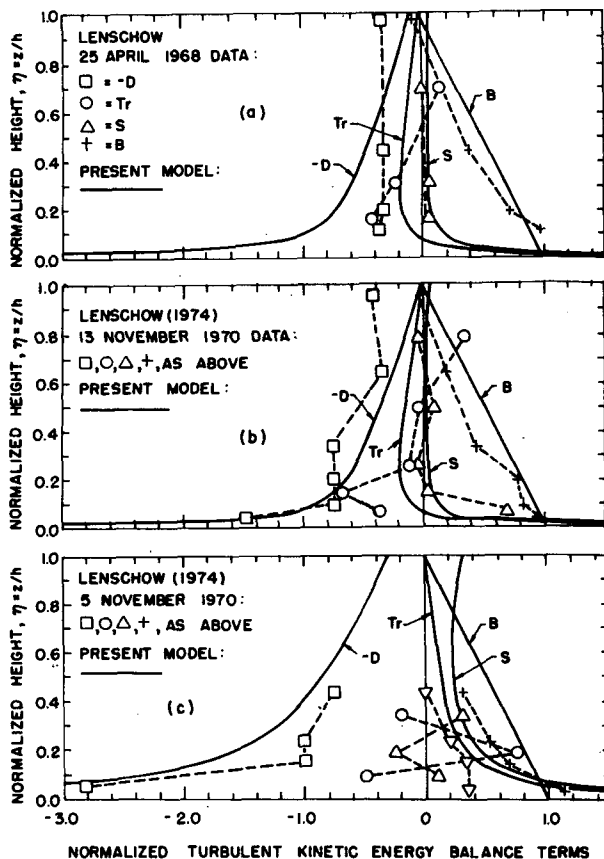


FIG. 6. Turbulent kinetic energy budget profiles. Similarity solutions of the quasi-steady Ekman model are compared with three sets of Lenschow's (1974) observations of convective PBL's using the bulk parameters of Table 3. The data points denoted ∇ on 5 November 1970 are a measured contribution to transport from advection.

Thus, while it is clear from the data of Wyngaard and Coté (1971), Pennell and Lemone (1974) and Lenschow (1974) that vertical diffusion is an energy loss (negative) near the surface of convective PBL's, it follows from the similarity functions of (25) that "transport" is positive. This can be seen in Fig. 7 of Wyngaard and Coté (1971) based on these functions which shows the imbalance term of opposite (positive) sign and greater magnitude than the diffusion term (called "turbulent transport" in this figure). Since our $Tr(\eta)$ is proportional to the algebraic sum of these divided by the positive surface buoyancy (in the convective case), a positive "transport" term near the surface of convective PBL's is expected, as shown in Fig. 6. On the other hand, our method for defining the closure functions in the upper PBL, while plausible and asymptotically correct at the surface, does not necessarily insure the proper balance of turbulent kinetic energy terms at the top, say, within an elevated inversion lid. In this connection we note Zilitinkevich's (1975b) recent observations on the importance of unsteady effects on "transport" in the vicinity of the

inversion layer. In principle, the present similarity formulation can be modified to account for a specified energy balance at the PBL top, possibly different from that implied by the present closure method. We shall not pursue this further here, however.

6. Concluding remarks

Our objective in this paper was to formulate a relatively simple, computationally economical model of the planetary boundary layer which accounts for most of the observational features of current interest. The early part of the paper deals with the formulation of a general similarity theory for the structure of entraining, buoyantly interactive, turbulent boundary layers, particularly those formed in first kilometer or so above the earth's surface.

For the general case we found the similarity profiles and bulk aerodynamic coefficients depend on similarity bulk parameters for surface roughness (h/z_0), buoyant stability of the turbulence near the surface (h/L), Coriolis effects (h/h_c), baroclinicity (h/x_0) and (h/y_0), and stability of the air mass overlying the PBL (h/z_0); and that a consistent similarity model with an entrainment surface at finite height forming the upper boundary may imply jumps or discontinuities in the flow variables. The jump conditions in the similarity model are the same as those derived for inversion lids by other authors.

As preliminary tests of the full similarity model, we compared the profiles computed with simplified versions against suitable field observations and laboratory experiments. The purpose of these tests was to check the properties of the turbulence closure model we derived from a combination of surface layer similarity theory and a special hypothesis which accounts for the observed variation of the turbulent scale or mixing length with distance above a surface. On balance, the comparisons are encouraging and suggest the full similarity formulation should be pursued. Eventually, this could well lead to an ordinary differential equation model which describes many of the observational features of interest in boundary layer meteorology. Such an approach would compliment multi-dimensional simulations, compensating for its lack of turbulence detail by computational economy, adaptability to parameterization, and possibly a more physically insightful representation of this interesting flow.

Acknowledgments. We thank Richard Somerville for suggesting the problem, and Gabriel Miller for his help with the similarity transformation. This work was initiated at the NASA Goddard Institute for Space Studies during the first author's tenure as NRC Senior Research Associate, and completed at the Department of Applied Science, New York University, under NASA Grant NSG-5045.

APPENDIX A

List of Symbols

B normalized buoyant production rate of turbulent kinetic energy
 $\{=[gF_b/(\rho C_p \theta_v)]/[gF_{bs}/(\rho C_p \theta_{vs})]\}$

c constant (≈ 0.052)

C_D drag coefficient $[=\tau_s/(\rho U_h^2)=(u^*/U_h)^2]$

C_E evaporative transfer coefficient
 $\{=-E_s/[\rho U_h(q_h-q_s)]\}$

C_H sensible heat transfer coefficient
 $\{=-F_s/[\rho C_p U_h(\theta_h-\theta_s)]\}$

C_p specific heat at constant pressure of air
 $[=7R/2 \approx 1000 \text{ J kg}^{-1} \text{ K}^{-1}]$

D normalized dissipation rate of turbulent kinetic energy $\{=\epsilon/[gF_{bs}/(\rho C_p \theta_{vs})]\}$

\bar{e} kinetic energy per unit mass in turbulent fluctuations $[=(\bar{u}'^2+\bar{v}'^2+\bar{w}'^2)/2]$

E vertical water vapor flux per unit area by turbulent fluctuations $[=\rho(\bar{w}'q')]$

f Coriolis parameter $[=2\Omega \sin\phi]$

F vertical sensible flux per unit area by turbulent fluctuations $[=\rho C_p(\bar{w}'\theta')]$

F_b vertical buoyancy flux per unit area by turbulent fluctuations $[=\rho C_p(\bar{w}'\theta'_b)]$

\hat{F}_b dimensionless buoyancy flux
 $[=-F_b/(\rho C_p u^* \theta'_b)]$

g gravitational acceleration at sea level ($\approx 9.81 \text{ m s}^{-2}$)

G vertical turbulent kinetic energy flux per unit area $[=\rho(\bar{w}'e')+(\bar{w}'p')]$

h overall boundary layer height or thickness

h_c Coriolis or Ekman layer scale height $[=\kappa u^*/f]$

K_H turbulent eddy diffusivity of sensible heat
 $[=-\overline{(w'\theta')}/(\partial\bar{\theta}/\partial z)]$

\hat{K}_H dimensionless eddy diffusivity for sensible heat
 $[=K_H/(\kappa u^* h)]$

K_m turbulent eddy diffusivity of momentum
 $[=-\overline{(u'w')}/(\partial\bar{u}/\partial z)=-\overline{(v'w')}/(\partial\bar{v}/\partial z)]$

\hat{K}_m dimensionless eddy diffusivity for momentum
 $[=K_m/(\kappa u^* h)]$

l turbulence mixing length scale $[=K_m^{3/2}\epsilon^{-1}]$

l_N turbulence mixing length scale under neutral conditions

\hat{l}_N dimensionless neutral mixing length $[=l_N/h]$

L Monin-Obukhov-buoyant stability lengthscale
 $[=\theta_{vs}u^{*2}/(\kappa g \theta'_v)]$

p air pressure

q specific humidity

R gas constant of dry air ($\approx 287 \text{ J kg}^{-1} \text{ K}^{-1}$)

Re_h Bulk Reynolds number $[=U_h h/\nu]$

Ri local gradient Richardson number
 $\{=[(g/\theta_{vs})\partial\bar{\theta}_v/\partial z]/[(\partial\bar{u}/\partial z)^2+(\partial\bar{v}/\partial z)^2]\}$

Ri_h bulk Richardson number
 $[=gh(\theta_{vh}-\theta_{vs})/(\theta_{vs}U_h^2)]$

S normalized shear production rate of turbulent kinetic energy
 $\{=[(\tau_x/\rho)(\partial\bar{u}/\partial z)+(\tau_y/\rho)(\partial\bar{v}/\partial z)]/[gF_{bs}/(\rho C_p \theta_{vs})]\}$

t time

T temperature

Tr normalized "transport" rate of turbulent kinetic energy
 $\{=-[(1/\rho)\partial G/\partial z+d\bar{e}/dt]/[gF_{bs}/(\rho C_p \theta_{vs})]\}$

u horizontal velocity in *x* direction

\hat{u} dimensionless horizontal velocity in *x* direction
 $[=\kappa\bar{u}/u^*]$

u_g geostrophic wind component in *x* direction
 $[=-\partial p/\partial y)/(\rho f)]$

\hat{u}_g dimensionless geostrophic wind in *x* direction
 $\{=\kappa u_g/u^*=-[h_c/(\rho u^{*2})]\partial p/\partial y\}$

*u** frictional velocity scale
 $[=(\tau_s/\rho)^{1/2}=(\overline{u'w'})_s^{1/2}]$

v horizontal velocity in *y* direction

\hat{v} dimensionless horizontal velocity in *y* direction
 $[=\kappa\bar{v}/u^*]$

v_g geostrophic wind component in *y* direction
 $[=(\partial p/\partial x)/(\rho f)]$

\hat{v}_g dimensionless geostrophic wind in *y* direction
 $\{=\kappa v_g/u^*=[h_c/(\rho u^{*2})]\partial p/\partial x\}$

w vertical velocity in *z* direction

w_e entrainment velocity $[=dh/dt-w_h]$

\hat{w}_e dimensionless entrainment velocity
 $[=w_e/(\kappa u^*)]$

*w** buoyancy velocity scale
 $\{=(-ghu^*\theta'_v/\theta_{vs})^{1/2}=[gh(\overline{w'\theta'_b})_s/\theta_{vs}]^{1/2}\}$

x horizontal intrinsic coordinate parallel to surface

x_g horizontal thermal gradient scale in *x* direction
 $\{=[u^{*2}/(gh)](\partial \ln(\theta_v)/\partial x)^{-1}\}$

y horizontal intrinsic coordinate normal to surface

y_g horizontal thermal gradient scale in *y* direction
 $\{=[u^{*2}/(gh)](\partial \ln(\theta_v)/\partial y)^{-1}\}$

z vertical coordinate

z₀ surface roughness length scale

z_g vertical scale for stability of air mass above PBL
 $\{=[u^{*2}/(gh)](\partial \ln\theta_v^+/\partial z)^{-1}\}$

α turbulence closure function $[=K_H/K_m]$

β turbulence closure function $[=l/l_N]$

γ turbulence closure function
 $[=-C_p\bar{\theta}_v(\rho d\bar{e}/dt+\partial G/\partial z)/(gF_b)]$

ε dissipation rate per unit mass of kinetic energy in turbulent fluctuations
 $[=\frac{1}{2}\nu \sum_{i,j} \overline{(\partial u'_i/\partial x_j+\partial u'_j/\partial x_i)^2}]$

ζ generalized stability variable $[=l_N/(\kappa L)]$; in the surface layer $\zeta \rightarrow z/L$

η similarity variable $[=z/h(t)]$

η₀ dimensionless surface roughness scale $[=z_0/h]$

θ	potential temperature [$=T(p_0/p)^{R/C_p} \approx T + gz/C_p$]
θ_v	virtual potential temperature [$\approx \theta(1+0.608q)$]
$\hat{\theta}_v$	dimensionless thermal variable [$=\kappa(\hat{\theta}_v - \theta_{vs})/\theta_v^*$]
θ_v^*	buoyancy thermal scale [$=-F_{bs}/(\rho C_p u^*) = -(\overline{w'\theta_v'})_s/u^*$]
κ	von Kármán's constant (≈ 0.35)
ν	molecular kinematic viscosity
ρ	air density
τ_x	Reynolds stress in x direction [$=-\rho(\overline{u'w'})$]
$\hat{\tau}_x$	dimensionless Reynolds stress in x direction [$=\tau_x/(\rho u^*{}^2)$]
τ_y	Reynolds stress in y direction [$=-\rho(\overline{v'w'})$]
$\hat{\tau}_y$	dimensionless Reynolds stress in y direction [$=\tau_y/(\rho u^*{}^2)$]
τ_s	Reynolds stress at the surface [$=\tau_x(z_0)$]
ϕ	latitude
ϕ_H	Monin-Obukhov function for buoyancy flux [$=(\kappa z/\theta_v^*)\partial\hat{\theta}_v/\partial z$]
ϕ_m	Monin-Obukhov function for shear [$=(\kappa z/u^*)\partial\bar{u}/\partial z$]
ϕ_ϵ	Monin-Obukhov function for dissipation [$=(\kappa z\epsilon)/u^*{}^3$]
Ψ_h	cross-isobar turning angle in quasi-steady Ekman model [$=\tan^{-1}(-v_h/u_h)$]
Ω	angular velocity of the earth's rotation ($\approx 7.29 \times 10^{-5}$ rad s^{-1})
∇	horizontal gradient operator [$=(\partial/\partial x, \partial/\partial y)$]
$()_h$	denotes conditions at $z=h$ immediately below discontinuity (when present)
$()_h^+$	denotes conditions in the free atmosphere immediately above discontinuity
$()_s$	denotes conditions at the surface $z=z_0$
$(-)$	denotes turbulent-mean value
$()'$	denotes turbulent fluctuation about the mean [$=() - (-)$]; also denotes differentiation with respect to the similarity variable [$=d()/d\eta$]
(\wedge)	denotes dimensionless quantity [defined in (15) and in this List of Symbols]
$\langle () \rangle$	denotes depth-averaged quantity

$$\left[= (1/h) \int_0^h () dz \right]$$

APPENDIX B

Closure Functions Near the Surface

The behavior of the turbulence closure functions near the surface can be derived in a consistent manner from relations associated with Monin-Obukhov (1953) surface layer similarity theory. In particular, the following relations are known to apply near the surface

($z_0 \leq z \ll h$):

$$\left. \begin{aligned} \tau_x &= \rho u^*{}^2, & F_{bs} &= -\rho C_p u^* \theta_v^*, & l_N &= \kappa z, \\ \partial\bar{u}/\partial z &= u^* \phi_m / l_N, & \partial\hat{\theta}_v/\partial z &= \theta_v^* \phi_H / l_N, & \epsilon &= u^*{}^3 \phi_\epsilon / l_N. \\ \zeta &= z/L = g l_N \theta_v^* / (\theta_v u^*{}^2). \end{aligned} \right\}$$

The corresponding eddy diffusivities, mixing length and Richardson number are

$$\left. \begin{aligned} K_m &= \frac{\tau_x/\rho}{\partial\bar{u}/\partial z} = \frac{u^* l_N}{\phi_m}, & K_H &= \frac{-F_{bs}/(\rho C_p)}{\partial\hat{\theta}_v/\partial z} = \frac{u^* l_N}{\phi_H} \\ l &= \frac{K_m^{1/2}}{\epsilon^{1/2}} = \frac{l_N}{\phi_m^{1/2} \phi_\epsilon^{1/2}}, & Ri &= \frac{g}{\theta_v} \frac{\partial\hat{\theta}_v/\partial z}{(\partial\bar{u}/\partial z)^2} = \frac{\zeta \phi_H}{\phi_m^2} \end{aligned} \right\}$$

The asymptotic form of the closure functions can now be evaluated. From (11a)

$$\alpha = K_H / K_m = \phi_m \phi_H^{-1}, \quad (A1)$$

from (11b)

$$\beta = l/l_N = \phi_m^{-1/2} \phi_\epsilon^{-1/2}, \quad (A2)$$

and from (9)

$$\begin{aligned} \gamma &= -1 + \frac{1}{\alpha Ri} \left(1 - \frac{K_m^2}{\beta^4 l_N^4 (\partial\bar{u}/\partial z)^2} \right) \\ &= -1 + (\phi_m - \phi_\epsilon) \zeta^{-1}. \end{aligned} \quad (A3)$$

REFERENCES

- Arya, S. P. S., 1975: Buoyancy effects in a horizontal flat-plate boundary layer. Part II. *J. Fluid Mech.*, **68**, 321-343.
- , and J. C. Wyngaard, 1975: Effect of baroclinicity on wind profiles and the geostrophic drag law for the convective boundary layer. *J. Atmos. Sci.*, **32**, 767-778.
- Bhumralkar, C. M., 1976: Parameterization of the planetary boundary layer in atmospheric general circulation models. *Rev. Geophys. Space Phys.*, **14**, 215-226.
- Blackadar, A. K., 1962: The vertical distribution of wind and turbulent exchange in a neutral atmosphere. *J. Geophys. Res.*, **67**, 3095-3102.
- Bobileva, I. M., S. S. Zilitinkevich and D. L. Laikhtman, 1967: Turbulent exchange in the thermally stratified planetary boundary layer. *Atmospheric Turbulence and Radiowave Propagation*, Nauka, 179-190 [in Russian].
- Businger, J. A., 1973: Turbulent transfer in the atmospheric surface layer. *Workshop on Micrometeorology*, Amer. Meteor. Soc., 67-100.
- , and S. P. S. Arya, 1974: Height of the mixed layer in the stably stratified planetary boundary layer. *Advances in Geophysics*, Vol. 18A, Academic Press, 73-92.
- , J. C. Wyngaard, Y. Izumi and E. F. Bradley, 1971: Flux-profile relationships in the atmospheric surface layer. *J. Atmos. Sci.*, **28**, 181-189.
- Carson, D. J., 1973: The development of a dry inversion-capped convectively unstable boundary layer. *Quart. J. Roy. Meteor. Soc.*, **99**, 450-467.
- Clarke, R. H., 1970: Observational studies in the atmospheric boundary layer. *Quart. J. Roy. Meteor. Soc.*, **96**, 91-114.
- , 1974: Attempts to simulate the diurnal course of meteorological variables in the boundary layer. *Izv. Akad. Nauk SSSR, Fiz. Atmos. Okeana*, **10**, 600-612.
- , A. J. Dyer, R. R. Brook, D. G. Reid and A. J. Troup, 1971: The Wangara experiment: Boundary layer data. Pap. No. 19, CSIRO Div. Meteor. Phys., 362 pp.

- Csanady, G. T., 1972: Geostrophic drag, heat and mass transfer coefficients for the diabatic Ekman layer. *J. Atmos. Sci.*, **29**, 488-496.
- , 1974: Equilibrium theory of the planetary boundary layer with an inversion lid. *Bound.-Layer Meteor.*, **6**, 63-79.
- Deardorff, J. W., 1972: Parameterization of the planetary boundary layer for use in general circulation models. *Mon. Wea. Rev.*, **100**, 93-106.
- , 1973: An explanation of anomalously large Reynolds stresses within the convective planetary boundary layer. *J. Atmos. Sci.*, **30**, 1070-1076.
- , 1974: Three-dimensional numerical study of the height and mean structure of a heated planetary boundary layer. *Bound.-Layer Meteor.*, **7**, 81-106.
- Donaldson, C. duP., 1973: Construction of a dynamic model of the production of atmospheric turbulence and the dispersal of atmospheric pollutants. *Workshop on Micrometeorology*, Amer. Meteor. Soc., 217-270.
- Dyer, A. J., 1967: The turbulent transport of heat and water vapor in an unstable atmosphere. *Quart. J. Roy. Meteor. Soc.*, **93**, 501-508.
- Heisenberg, W., 1948: Zur statistischen Theorie der Turbulenz. *Z. Phys.*, **124**, 628-657.
- Hess, S. L., 1959: *Introduction to Theoretical Meteorology*. Holt, Rinehart and Winston, 362 pp.
- Lenschow, D. H., 1974: Model of the height-variation of the turbulence kinetic energy budget in the unstable planetary boundary layer. *J. Atmos. Sci.*, **31**, 465-474.
- Lilly, D. K., 1968: Models of cloud-topped mixed layers under a strong inversion. *Quart. J. Roy. Meteor. Soc.*, **94**, 292-309.
- Lumely, J. L., and B. Khajeh-Nouri, 1974: Computational modeling of turbulent transport. *Advances in Geophysics*, Vol. 18A, Academic Press, 169-192.
- Mahrt, L., and D. H. Lenschow, 1976: Growth dynamics of the convectively mixed layer. *J. Atmos. Sci.*, **33**, 41-51.
- Melgarejo, J. W., and J. W. Deardorff, 1974: Stability functions for the boundary layer resistance laws based on observed boundary layer heights. *J. Atmos. Sci.*, **31**, 1324-1333.
- Mellor, G. L., and T. Yamada, 1974: A hierarchy of turbulence closure models for the planetary boundary layer. *J. Atmos. Sci.*, **31**, 1791-1806.
- Monin, A. S., and A. M. Obukhov, 1953: Dimensionless characteristics of turbulence in the atmospheric surface layer. *Dokl. Akad. Nauk SSSR*, **93**, 223-226.
- , and A. M. Yaglom, 1971: *Statistical Fluid Mechanics: Mechanics of Turbulence*, Vol. 1. The MIT Press, 769 pp.
- Orlanski, I., B. B. Ross and L. J. Polinsky, 1974: Diurnal variations of the planetary boundary layer in a mesoscale model. *J. Atmos. Sci.*, **31**, 965-989.
- Pennell, W. T., and M. A. Lemone, 1974: An experimental study of turbulence structure in the fair weather trade wind boundary layer. *J. Atmos. Sci.*, **31**, 1308-1323.
- Prandtl, L., 1925: Bericht über Untersuchungen zur ausgebildeten Turbulenz. *Z. Angew. Math. Mech.*, **5**, No. 2, 136-139.
- , 1932: Meteorologische Anwendungen der Strömungslehre. *Beitr. Phys. Atmos.*, Bjerkness Festschrift, **19**, No. 3, 188-202.
- Sarachik, E. S., 1974: The tropical mixed layer and cumulus parameterization. *J. Atmos. Sci.*, **31**, 2225-2230.
- Schlichting, H., 1960: *Boundary-Layer Theory*. McGraw-Hill, 647 pp.
- Sheppard, P. A., 1970: The atmospheric boundary layer in relation to large-scale dynamics. *The Global Circulation of the Atmosphere*, Roy. Meteor. Soc., 91-112.
- Tennekes, H., 1973: A model for the dynamics of the inversion above a convective boundary layer. *J. Atmos. Sci.*, **30**, 558-567.
- Wippermann, F. K., 1974: Eddy diffusion coefficients in the planetary boundary layer. *Advances in Geophysics*, Vol. 18A, Academic Press, 407-418.
- Wyngaard, J. C., and O. R. Coté, 1971: The budgets of turbulent kinetic energy and temperature variance in the atmospheric surface layer. *J. Atmos. Sci.*, **28**, 190-201.
- , and —, 1974: The evolution of a convective planetary boundary layer: a higher-order-closure model study. *Bound.-Layer Meteor.*, **7**, 289-308.
- Zeman, O., 1975: The dynamics of entrainment in the planetary boundary layer: A study in turbulence modeling and parameterization. Ph.D. thesis, Pennsylvania State University, 216 pp.
- Zilitinkevich, S. S., 1970: *Dynamics of the Atmospheric Boundary Layer*. Hydrometeorological Press, 290 pp. [in Russian].
- , 1975a: Resistance laws and prediction equations for the depth of the planetary boundary layer. *J. Atmos. Sci.*, **32**, 741-752.
- , 1975b: Comments on "A model for the dynamics of the inversion above a convective planetary boundary layer". *J. Atmos. Sci.*, **32**, 991-992.
- , and J. W. Deardorff, 1974: Similarity theory for the planetary boundary layer of time-dependent height. *J. Atmos. Sci.*, **31**, 1449-1452.